Coupling Modes in Supersonic Twin Rectangular Jets

Ata Esfahani*, Nathan Webb†, and Mo Samimy‡
Gas Dynamics and Turbulence Laboratory, Aerospace Research Center
The Ohio State University, Columbus, Ohio 43235

AIAA SciTech 2021 Meeting
January 11th-15th 2021

In the closely spaced twin-jet configuration often seen in military aircraft, the jets can become coupled, resulting in significantly increased near-field pressure fluctuations and far-field noise. The propulsion/airframe integration benefits of non-axisymmetric nozzles has led to renewed interest in their integration into future generations of aircraft design. A thorough understanding of the coupling dynamics and their effects on screech amplitude, intense near-field unsteady pressure fluctuations and far-field noise levels and directivity is needed to effectively implement active flow control strategies to disrupt the underlying mechanisms of coupling. The results of experiments aimed at characterizing the coupling modes of closely spaced, low aspect ratio, twin rectangular supersonic jets with a design Mach number 1.5 are presented in this paper. The results of near-field experiments indicate that anti-symmetric screech modes are present in both overexpanded and underexpanded flow regimes. The results also indicate that the jets, in general, are coupled out-of-phase along the minor axis of the jets in the overexpanded regime and in-phase in the underexpanded regime. Flow visualization with a Z-type schlieren system showed that the jet spreading angle in the vertical plane is higher when the jets are coupled out-of-phase. Visualization experiments also showed that standing waves are present at Mach numbers where the screech amplitude and coherence are increasing. More work is needed to understand the interplay between standing waves and the strength of screech.

I. Nomenclature

AR	=	nozzle aspect ratio
$BBSAN$	=	broadband shock-associated noise
D_e	=	area-based equivalent nozzle diameter
f	=	screech frequency
M_d	=	design Mach number
M_j	=	fully expanded jet Mach number
NPR	=	nozzle pressure ratio
s	=	nozzle center-to-center spacing in a twin-jet setup
SPL	=	sound pressure level in dB
St	=	screech Strouhal number, fD_e/u_j
θ	=	polar angle
ρ	=	near-field density
σ	=	standard deviation
φ	=	azimuthal angle

* PhD Student, Department of Mechanical and Aerospace Engineering, AIAA student member
† Research Scientist, Aerospace Research Center, AIAA Senior Member
‡John B. Nordholt Professor of Mechanical and Aerospace Engineering, AIAA Fellow, Corresponding Author: samimy.1@osu.edu

II. Introduction

The propulsion/airframe integration benefits of non-axisymmetric nozzles has led to renewed interest in their integration into future generations of aircraft design. The evolution of exhaust system design requirements in response to a need for greater operational performance led to the rise of additional requirements such as minimizing drag, thrust reversing, thrust vectoring in pitch, yaw and roll and improved flow mixing [1]. Integration of the aft body and nozzle in an aircraft can severely affect drag and weight. Since the aft body of an aircraft is not typically axisymmetric, integrating an axisymmetric nozzle with the airframe would introduce additional drag [2]. As a result, non-axisymmetric nozzles are an attractive option for minimizing drag. Studies have shown [3,4] that the plume spreading rate of a rectangular nozzle can be significantly higher than that of an equivalent axisymmetric nozzle. It is also easier to implement a thrust vectoring system in a two-dimensional nozzle as the nozzle walls can simply be deflected to provide thrust vectoring in pitch, yaw or even roll axis in addition to thrust reversing functions. Furthermore, a 4-flap, two-dimensional nozzle system can be lighter than an equivalent axisymmetric design [1]. Aircraft with high- and low-aspect-ratio nozzles have already been operational for years and recent interest in developing manned and unmanned platforms with non-axisymmetric nozzles integrated with the airframe (e.g. F/A-XX, MQ-25 and X-47 programs, see Fig. 1) underscores the need for further development and characterization of such geometries. Another issue that needs to be considered when designing future aircraft with twin rectangular nozzles that improve propulsion/airframe integration is sonic/acoustic fatigue [5]. Due to widespread use of composites and special stealth coatings in the latest generation of high-performance military aircraft, structural components in the vicinity of the nozzles must be protected from the high levels of fluctuating pressures caused by coupling of the jets [6–8].

Fig. 1. Various Navy program demonstrators employing non-axisymmetric nozzle designs a) Boeing F/A-XX rendering b) Northrop Grumman X-47B c) Boeing MQ-25

Despite the need for better understanding and characterizing the flow in twin rectangular geometries, it is surprising to see that only a handful of studies have been directed at this topic over the past three decades. A list of studies covering the topic of twin rectangular jets is provided in Table 1. The earliest work on the coupling between two low aspect ratio rectangular jets was reported by Zilz and Wlezien [9]. The authors identified the four possible coupling modes between low aspect ratio rectangular jets arranged side-by-side along their major axes: normal symmetric (in-phase coupling in the vertical plane), normal asymmetric (out-of-phase coupling in the vertical plane), lateral symmetric and lateral anti-symmetric (out-of-phase and in-phase coupling in the horizontal plane, respectively). They also noted that symmetric coupling modes generate higher sound pressure levels (SPL) whereas anti-symmetric modes led to a reduction in SPL in the plane of symmetry. Zilz and Wlezien reported that anti-symmetric modes are present in closely spaced, underexpanded jets. Another notable finding of their study was the fact that higher spreading rates in rectangular jets can lead to rapid merging of the plumes and result in screech suppression. Following their work, Zeierman et al [10] studied the spreading rates of plumes in two adjacent rectangular nozzles with an aspect ratio of 3. They found that operating twin nozzles above their design Mach number does not alter the spreading rate compared to a single rectangular nozzle. However, when operated at a highly overexpanded condition, there is a significant increase in plume diffusion rate due to the addition of the second jet.

Raman and Taghavi [11] performed a comprehensive study of coupling between twin rectangular jets. The aspect ratio in their work was 5, and the work itself is an extension of their earlier study of coupling between a linear array of four jets [12]. In their work, while looking at mixing and noise benefits, Raman and Taghavi [8] synchronized the four jets to achieve higher mass flux and plume spreading rates. In their follow-up study [11], Raman and Taghavi confirmed the findings of Zilz and Wlezien [9], namely that anti-symmetric flapping of the jets minimizes the near-field pressure fluctuation levels (at $\varphi = 90°$) and symmetric flapping maximizes them.

Two more recent studies by Bozak [9] and Bozak and Wernet [14] were aimed at developing an empirical model for prediction of noise in twin circular and rectangular nozzles. They also studied flow velocity in the inter-nozzle region with PIV and noted that the addition of forward-flight effects led to the creation of a low velocity region

between the two nozzles which, in turn, led to higher turbulent kinetic energy levels for the jet and an increase in the far-field sound pressure level (SPL) [14].

Table 1. List of studies on planar, twin rectangular jets (*s*: center-to-center nozzle spacing, *h*: nozzle exit height, *w*: nozzle exit width, D_e: nozzle exit equivalent diameter)

Author	Nozzles Design	Nozzle Spacing	Range of Mach Numbers Investigated
Zilz and Wlezien, 1990	C-D, rectangular M_d = 1.25, 1.45 AR = 1.15, 2.86	s/w = 1.55 – 3.2	M_j = 1.26 – 1.55
Walker, 1990	C-D, rectangular M_d = 1.40 AR = 3.71	s/w = 2.50 – 3.7	M_j = 1.1 – 1.7
Zeierman et al., 1992	C-D, rectangular M_d = 1.8 AR = 3	s/D_e = 1 – 4	M_j = 1.6 – 2.1
Raman and Taghavi, 1996	Converging nozzles, AR = 5	s/h = 4, 5.5, 7.5, 10, 11.5, 13.7	M_j = 1.2 – 1.75
Raman and Taghavi, 1998	Converging nozzles, AR = 5	s/h = 5.5, 9, 15	M_j = 1.0 – 1.6
Bozak, 2014	Converging nozzles, AR = 2, 8	s/D_e = 2.45, 3.32, 5.26	M_j = 0.9 – 1.33

Almost all of the previous studies, with the works of Zilz and Wlezien [9] and [15] being an exception, have been directed towards investigating high aspect ratio nozzles with significant inter-nozzle spacings, a combination which may not be of interest for airframe/propulsion integration in the latest generation of tactical manned and unmanned aircraft. While a significant body of work on the physics and control of twin circular jets exists in the literature (e.g. recent work in our laboratory [16]) no attempt has been made, to the authors' knowledge, to control and decouple twin rectangular jets with active flow control techniques. The use of passive techniques, such as installing tabs in the nozzles, to decouple twin rectangular jets has resulted in very limited success as reported by Walker [11]. A thorough understanding of coupling modes between the jets is needed in order to implement active flow control strategies that would disrupt the underlying mechanisms of coupling. The works published recently on low aspect ratio, closely-spaced twin rectangular jets [17–19] have not investigated coupling between the jets across the wide range of NPRs likely present in application.

The work presented here fills this gap in the literature by investigating a pair of closely spaced, low aspect ratio rectangular nozzles at multiple NPRs. The objective of this work is to characterize coupling between the jets and the near-field dynamics and far-field noise at various operating regimes (from highly overexpanded to underexpanded) and establish a baseline for future experiments aimed at controlling the jets using Localized Arc Filament Plasma Actuators (LAFPAs). LAFPAs have been developed at the Gas Dynamics and Turbulence Laboratory (GDTL) [20,21] and have been implemented in various jets [18], including twin supersonic circular jets [12]. These actuators exert control authority by producing periodic thermal perturbations using an arc discharge. The perturbations excite the Kelvin-Helmholtz instability in shear layers of the jet, and the amplified perturbations eventually roll up into flow structures. By modifying the frequency and relative timing of the LAFPAs perturbations, the spatial organization and growth of flow structures can be controlled [22]. Large-scale structures are known to play a critical role in mixing and acoustics in jet flows [14]. Thus, the LAFPAs can, using only perturbation-frequency inputs, exert significant control authority over jets and other flows with shear layers[23–27]. More details on the mechanism through which LAFPAs excite the flow can be found in a recent review article by Samimy et al. [28]. An understanding of dynamics and the interplay between various phenomena such as screech, coupling, and standing waves is crucial to leveraging the

naturally occurring instabilities that can generate the desired flow control effects. This paper details the facility design and characterization, along with physics of coupling in the near-field and its effects on far-field SPL and directivity.

III. Experimental Methodology

A. Nozzle Design

A new nozzle assembly was designed and built at the GDTL to study flow physics and aeroacoustics of low aspect ratio, twin supersonic rectangular jets. The assembly uses a pair of sharp throated, military style rectangular converging-diverging nozzles with a design Mach number of 1.5 (M_d = 1.5) and aspect ratio of 2 (AR = 2). From the outset, the assembly was designed to be modular to accommodate possible changes in nozzle spacing, design Mach number and actuator configuration by replacing specific parts with alternate versions.

In its current configuration, the nozzle exit width (w), height (h) and aspect ratio (AR) are 24.13 mm, 12.06 mm and 2, respectively. The center-to-center spacing between the nozzles is 43.38 mm (2.25D_e). The area-based equivalent diameter is D_e = 19.25 mm. A cross section of the nozzle assembly can be seen in Fig. 2a.

Boron nitride housings for LAFPAs ("actuator blocks") are used to house the plasma actuators and prevent arcing to metal parts. In order stabilize the arc in the upcoming flow control experiments and allow its frequency to be precisely controlled, 1 mm wide by 0.5 mm deep grooves were cut into the actuator block, approximately 1 mm upstream of the nozzle exit plane. The 1 mm diameter tungsten electrode tips are contained within the groove and held flush with the jet inner surface. Previous work [29] has shown that the existence of the groove does not affect the control authority of the actuators. The actuators and the grooves are present in the baseline geometry examined in this paper to ensure that the upcoming excited flow results are compared to baseline results from an identical geometry.

Figure 2b shows a cutaway of the actuator block depicting the electrode bores and setscrew holes that are present in the baseline cases reported here. The nozzle assembly (Fig. 3a) is attached to a high-pressure air pipe at the center of a co-flow duct (Fig. 3b), used for simulating forward flight effects, via a circular mounting plate. A custom designed metallic O-ring between the interface of the nozzle assembly and mounting plate ensures a tight seal exists between these parts even during heated flow experiments.

Following the installation of the new nozzle assembly in the anechoic chamber at the GDTL a Mach number sweep in increments of 0.05 was conducted between M_j = 1.4 and M_j = 1.6 in order to determine the ideally expanded Mach number of the new facility. The far-field array was used to collect the data at an azimuthal angle of 90° (φ = 90° see Fig. 3a) and polar angles of 30°, 90° and 120°. The shape of the spectra, specifically the amplitude of the screech tones and broadband shock associated noise (BBSAN) peaks, were analyzed to infer the ideally expanded flow case. The presence of a shock system, originating from the nozzle throat, in addition to a shock cells present in non-ideally expanded cases complicates the task of interpreting the spectra and establishing the ideally expanded case. Nevertheless, based on the trends seen in the spectra (not shown here), we determined that the ideally expanded Mach number is very near the design Mach number of $M_d = M_j$ = 1.50.

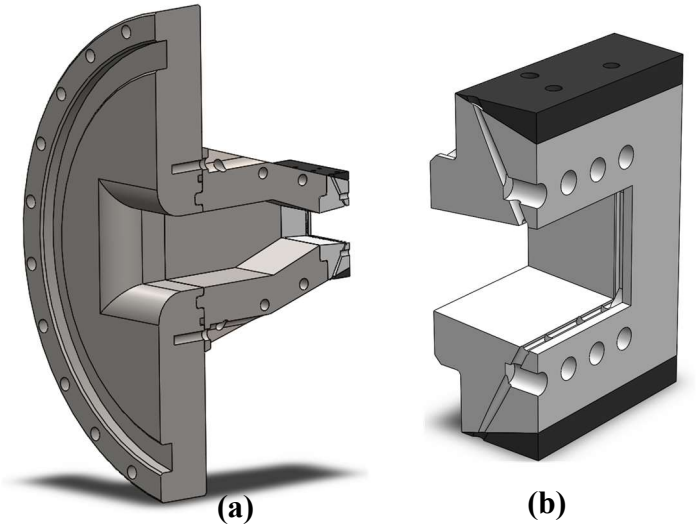

Fig. 2. a) Nozzle cross-section, b) actuator block cutaway

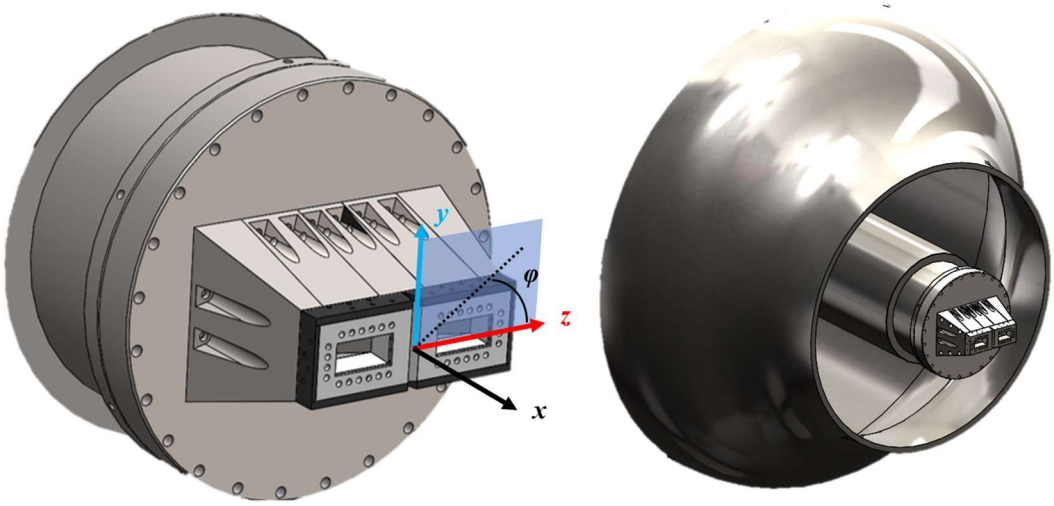

(a) **(b)**

Fig. 3. a) Twin-jet assembly showing minor axis, *y*, major axis, *z*, and azimuthal angle, *φ*; b) twin-jet nozzle assembly installed inside the co-flow channel

B. Facility and Instrumentation

All the experiments reported in this work have been conducted in the jet anechoic facility at the GDTL within the Aerospace Research Center at the Ohio State University. The facility is a 6.2 m × 5.6 m × 3.4 m anechoic chamber with a cut-off frequency of 160 Hz. High-pressure air is supplied by three five-stage reciprocating compressors that store the air in two cylindrical tanks with a total storage capacity of 43 m^3 at a maximum pressure of 16 MPa. The air is then dried, filtered and passed through a series of screens in the settling chamber before being fed to the jet plenum. A computer-controlled valve maintains the plenum pressure at a setpoint to maintain a constant NPR The nozzle assembly is attached to the plenum using a circular mounting plate to allow the azimuthal angle of the nozzle assembly (φ) with respect to the far-field microphone array to be adjusted in 15° increments. The facility is capable of heating the air in the stagnation chamber up to a total temperature ratio of 2.5. Forward flight conditions can be simulated using a co-flow duct that can provide a stream of air at up to 100 m/s. The co-flow duct and the twin-jet nozzle assembly were covered with acoustic foam (as seen in Fig. 4) during the experiments to prevent acoustic reflections.

A series of experiments at various nozzle pressure ratios (*NPRs*), ranging from moderately overexpanded (M_j = 1.2) to moderately underexpanded (M_j = 1.85) flow regimes, was conducted. This paper focuses on three jet operating conditions that represent different jet behaviors observed in the course of our detailed investigation of low aspect ratio twin rectangular jets. Near- and far-field acoustic data and schlieren images were acquired for *NPR* of 2.97, 3.67, and 5.0, corresponding to the following fully expanded jet Mach numbers (M_j): 1.35, 1.50, and 1.70, all at a jet total temperature ratio of 1. These three *NPR*s correspond to an overexpanded case, an ideally expanded case and an underexpanded case.

A near-field array, consisting of a 38 cm × 38 cm rectangular frame and six Brüel and Kjær 4939 $\frac{1}{4}$ in. microphones, was used to collect data to study the coupling between the jets at various regimes. By computing the coherence and phase difference between the pressure traces from individual microphones in the array, it is possible to assess the coupling and screech modes of the jets at different operating Mach numbers. The number of microphones was chosen so that it would be possible to infer both the screech mode of each jet [30,31] and the coherence and phase of the jets with respect to each other, as reported by Raman and Taghavi [11]. All of the near-field microphones were positioned at an axial location of x/D_e = 0 and radially (measured from the nearest jet centerline) at r/D_e = 4. These axial and radial distances are sufficiently far from the jet boundary to be free of the hydrodynamic signature of the jet and record only the acoustic signature of screech. The array and microphone mounts were wrapped in acoustic foam to prevent reflections, as seen in Fig. 4. The array microphones were numbered in a counterclockwise (looking upstream) fashion starting with the right horizontal microphone.

A schematic of the far-field microphone array is shown in Fig. 5. Eight Brüel and Kjær 4939 $\frac{1}{4}$ in. microphones mounted at polar angles (θ), ranging from 30° to 120°, measured from the downstream jet axis, are aimed at the midpoint between the centerline of the twin-jet nozzles and are used to collect far-field data. The individual microphone distances from the jet centerline range from 1.90 *m* to 3.78 *m* (98.9D_e to 196.5D_e). The results were propagated to an observer distance of 100D_e from the point centered between the two jets along the major axis.

A standard Z-type schlieren system was used to visualize the flow-field along the major and minor axes of the jets. To acquire high-resolution, time-averaged maps of density gradient at a wide range of Mach numbers, a 5.5 MP LaVision Imager sCMOS camera was used. The knife edge was oriented vertically in order to highlight the horizontal density gradients and 300 images with a window size of 2500×2150 pixels were acquired at 50 frame per second for each test condition. An HPLS-36 high-powered pulsed LED from Lightspeed Technologies was used as the light source. The LED pulse width was set to 500 *ns* which was short enough to freeze the flow features even for the highest observed screech frequency. The Imager sCMOS camera was swapped with a Phantom v1210 camera for high-speed schlieren imaging experiments. The goal of these experiments was to capture the motion of the screeching jets at various Mach numbers. The frame acquisition rate was fixed at 60,000 frames per second for all the tested Mach numbers and a set of 1000 frames with a window size of 512×340 pixels was recorded for each case. A Nikon zoom lens was used to set the field of view to include only the flow features of interest, namely the shock system while reducing the window size to allow an increase in maximum frame rate.

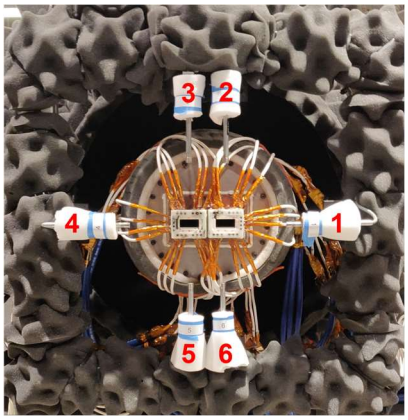

Fig. 4. Photograph of near-field microphone array covered with foam to prevent acoustic reflections

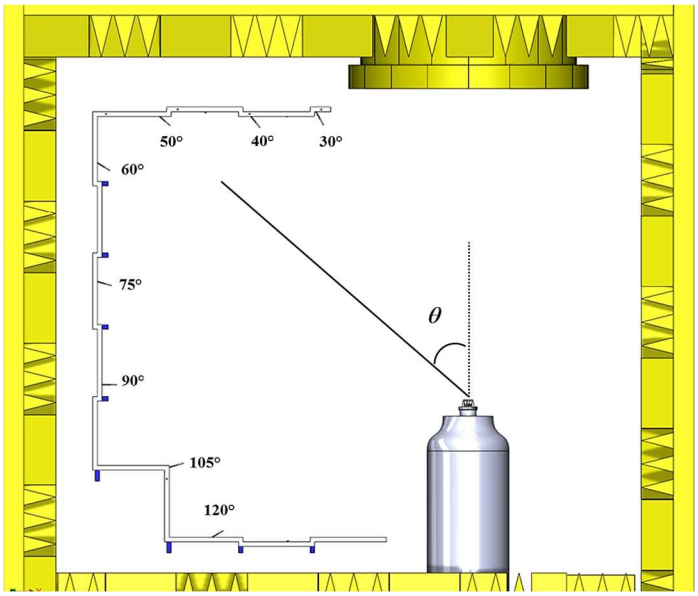

Fig. 5. Schematic of far-field microphone array and polar angle, θ

C. Data Acquisition and Processing

Near- and far-field acoustic signals collected by microphones were amplified and band-pass filtered between 20 Hz and 100 *kHz*, with Nexus 2690 signal conditioners. Prior to acquiring a set of near-field or far-field data, an experiment was conducted to ascertain the appropriate level of gain. Microphone calibrations were then performed at the set gain values using a Brüel and Kjær model 4231 acoustic calibrator. The sampling frequency was 200 *kHz.* For near-field acoustic measurements, 100 blocks of 32,768 samples were acquired for each data point while for far-field measurements 400 blocks of 8,192 samples were recorded for each test case. These acquisition parameters result in a 24.4 *Hz* frequency resolution for the far-field results. The calculated Power Spectral Density plots are expressed as sound pressure level in decibels referenced to 20 μPa. As was mentioned earlier, the far-field results were propagated to an observer distance of $100D_e$ assuming a spherical propagation.

The jet screech and coupling modes were determined from the relative phase and coherence of the signals acquired from various near-field microphones. In order to extract this information wavelet (Morlet) coherence and phase between various pairs of microphone signals were calculated. The temporal averages of the coherence and phase are performed using only time instants with a coherence greater than 0.7. This allows the average phase of the signals to be examined only when the coherence values are high (and therefore the phases are reliable).

Maps of average density gradients and standard deviation of density gradients were calculated from the time-averaged schlieren images in DaVis 8.2 and then imported in MATLAB where Log_{10} of standard deviation of density gradients was computed and plotted to visualize the standing wave patterns at various Mach numbers.

IV. Results and Discussion

The purpose of this paper is to present the results of experiments aimed at characterizing the baseline of a low aspect ratio twin rectangular supersonic jets. Understanding the underlying physics of coupling in the baseline case will enable us to implement effective flow control strategies.

A. Acoustic Measurements

1. Near-field Results

A detailed, fully-expanded jet Mach number sweep was conducted to obtain screech frequency in both overexpanded and underexpanded jet operating regimes. Various scaling parameters for the screech frequency were explored and it was found that the normalized screech frequencies using the geometrical nozzle exit equivalent diameter and fully expanded jet velocity ($St = fD_e/u_j$) collapse the data from our experiments as well as data from other researchers using rectangular jets with small ($AR = 2$) to moderate ($AR = 5$) aspect ratios. Figure 6 shows a comparison between the screech tones reported by Shih et al. [34], Panda et al. [35], Raman [36], Alkislar [3], Karnam et al. [32] and our results. Our data points presented in Fig. 6 have been acquired using the near-field microphone array and compared with spectra from data gathered simultaneously with far-field microphones located at $\theta = 30°$, 90° and 120° to ensure that screech tone frequencies are accurate. Surprisingly, the data collapse is good given that the results include both jets issuing from converging and converging-diverging nozzles and both single and twin-jet arrangements. Of greatest importance is the twin-jet setup investigated by Karnam et al. [32] and numerically simulated by Jeun et al. [33] and Viswanath et al [19] as these geometries are very similar to that investigated in this paper. Additionally, a survey of the literature was conducted to gather screech data from single and twin rectangular jets with various aspect ratios for comparison with the present results. Shih et al. [34] studied the variation of screech Strouhal number, when normalized using nozzle exit height (h), against M_j from the results of several authors and concluded that the variation of normalized screech tones against M_j is independent of nozzle aspect ratio. We investigated this finding using two scaling parameters, namely h and D_e, to collapse the screech data. The scaling parameter D_e was found to result in the best data collapse for low to moderate nozzle aspect ratios. However, the data from high aspect ratio nozzles (e.g. $AR = 10$, 16.7 [4], $AR = 9.63$[31]) do not collapse either with each other or with the results from low to moderate aspect ratio nozzles, i.e. $AR = 2 – 5$, regardless of whether h or D_e are used for normalization. To avoid cluttering the graph, results from the higher aspect ratio nozzles are omitted from the figure below.

Although the general collapse of the data from nozzles with a relatively wide range of aspect ratios and internal geometries (converging or converging-diverging) and single or twin jets is good, it is instructive to observe that the screech data from converging-diverging nozzles show more scatter in the overexpanded regime but demonstrate better collapse at underexpanded Mach numbers. We have also observed more day-to-day variations in screech peak

frequency in our own results at overexpanded Mach numbers. More research is needed to examine this issue. However, it should be noted that in the overexpanded flow regime, the nozzle exit pressure is lower than ambient pressure and an oblique shock wave is attached to the nozzle exit. Depending upon the strength of the pressure gradient at the nozzle exit, the boundary layer inside the nozzle could separate and introduce unsteadiness to the flow, shock system, and screech process. Furthermore, when the high *AR* cases (not included in this figure) are considered, a trend of higher *St* number for a given M_j with *AR* is observed, which shows that the relevancy of D_e as a length scale is reduced as *AR* is increased.

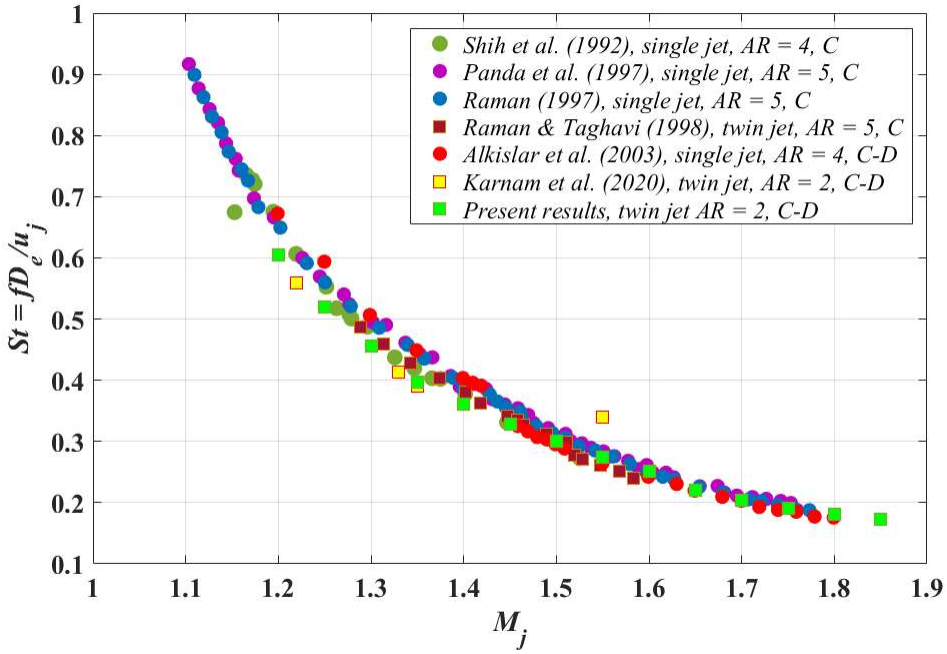

Fig. 6 Variation of screech Strouhal number vs. Mach number

As mentioned earlier, a thorough understanding of the coupling dynamics and mode at different Mach numbers is critical in implementing active flow control in order to reduce noise levels or decouple the jets. An extensive experimental campaign, aimed at characterizing the jets' coupling modes at a wide range of Mach numbers was conducted. All the results presented in this section have been acquired using the near-field microphone array described in section III.B. Time-averaged wavelet coherence and phase between near-field acoustic results are presented in Fig. 7. In order to infer the coupling mode of the jets, phase difference and coherence between signals from microphones 2 and 3 (see Fig. 4) were calculated and are presented in Fig. 7a. The jets start screeching for the first time at M_j = 1.20. The coherence between the jets increases progressively as the Mach number increases to the design Mach number, except for a dip at M_j = 1.25. A screech frequency mismatch between jets is observed only at lower overexpanded Mach numbers (i.e. M_j = 1.20 – 1.35). While initially the difference in screech frequencies between the jets is approximately 140 *Hz* at M_j = 1.20, it decreases to 33 *Hz* (its minimum value) as M_j increases to 1.35. This frequency mismatch causes the relative phase between the jets drifts in time which complicates the task of calculating a time-averaged value for phase difference. This phenomenon is further discussed below. As Mach number increases from M_j = 1.40 to 1.50, the frequency mismatch disappears and the coherence between the jets maintains its high value, leading to a steady phase difference between the jets at approximately $\pm\pi$. This indicates out-of-phase coupling. The general upward trend in coherence in the overexpanded regime with increasing Mach numbers is, in large part, caused by the screech intermittency at the low Mach numbers (M_j = 1.20 to 1.35), which results in alternately high and low coherence levels. The higher Mach numbers, as already mentioned, produce consistent screech and long periods of sustained high coherence. As a result, the time averaged coherence levels between M_j = 1.20 to 1.30 are lower than those of M_j = 1.40 to 1.50 (see Fig. 7a). After reaching the design Mach number, further increasing the Mach number causes an immediate drop in time-averaged coherence value at M_j = 1.55 (Fig. 7a), followed by screech strength augmentation and increases in coherence between the jets. In this regime, the jets are strongly coupled in-phase as indicated by the 0° phase difference between the jets (see Fig. 7a).

It is worth mentioning that while Zilz and Wlezien [9] and Walker [15] have reported the existence of lateral flapping in the horizontal plane (for low aspect ratio nozzles), we did not observe any evidence of coupling between the jets in the horizontal plane (major axis). These observations were reinforced by high-speed schlieren imaging experiments (not reported in this paper) which did not show any evidence of lateral flapping or coupling between the jets in the horizontal plane.

It is instructive to examine the coherence and phase difference between signals from microphones located above and below each jet (Fig. 7b). While examining coherence and phase difference between microphones 2 and 3 reveals the nature of coupling between the jets, the relative strength of coherence and phase difference between microphones 2 and 6, and 3 and 5 indicates the nature (i.e. screech is anti-symmetric or symmetric) as well as coherence of the screech of each jet. As we can see in Fig. 7b, the general trends in coupling strength are reflected in the coherence of the screech of each jet. High coherence for each individual jet at M_j = 1.35 – 1.45 and 1.70 – 1.85 is accompanied by strong coupling between the jets. It is also interesting to see that the coupling strength between the jets is almost never significantly higher than the coherence level of either of the jets. At Mach numbers where a frequency mismatch exists between the jets, i.e. M_j = 1.20 – 1.35, significant differences between the coherence level of the jets exist in some cases. Such significant differences are not observed at any Mach number in the underexpanded regime.

Having examined the coupling behavior of the jets for a wide range of Mach numbers, we can now move on to study the screech mode of each individual jet. Gutmark et al. [30], Shih et al. [34] and Raman and Rice [31] have noted that single rectangular jets can display either a flapping motion, also known as an anti-symmetric mode, or a pulsating movement in the axial direction which is commonly referred to as a symmetric mode. A plot of coherence and phase difference between microphones 2 and 6 positioned above and below the right jet is presented in Fig. 7c. In contrast to the coupling between the jets where values of time-averaged phase difference between microphones 2 and 3 were somewhat ambiguous at low overexpanded Mach numbers due to phase drift, it is interesting to see that for nearly all the Mach numbers tested, the time-averaged phase differences are close to $\pm\pi$ (see Fig. 7c). Even at Mach numbers where coherence in the jet on the right is relatively low, e.g. M_j = 1.20, 1.30, 1.50 and 1.65, the phase difference is close to $\pm\pi$. This indicates a strong flapping motion that is present throughout the test envelope. The results from Fig. 7a and c indicate that in general, the jets tend to display a flapping motion (anti-symmetric screech mode) and in overexpanded regime are largely coupled out-of-phase and in underexpanded regime are generally coupled in-phase. While some authors have observed both anti-symmetric and symmetric screech modes in their single jet experiments [30,31,34], our results are more in line with Raman and Taghavi's observations in a high aspect ratio twin-jet setup where they only observed an anti-symmetric screech mode for each jet [11].

The trends in near-field screech amplitude closely follow those of coherence between microphones 2 and 6 as shown in Fig. 7d. The amplitudes of screech peaks from time-averaged spectra recorded by microphone 2 are plotted over time-averaged coherence values in Fig. 7d. Raman and Taghavi [11] reported a 20 dB increase in the near-field screech amplitude as their high aspect ratio twin-jets switched from out-of-phase flapping to in-phase flapping. They also reported a significant reduction in screech amplitude in out-of-phase flapping mode compared to a single jet screech amplitude and observed a modest tone amplification for in-phase mode cases compared to their single-jet measurements. Zilz and Wlezien [9] also noted a 15 dB increase in screech tone amplitude as the their twin jets switched from out-of-phase coupling to in-phase coupling while Walker [15] observed insignificant differences in screech amplitudes as jets switched modes. While we do not have any single jet data available at this time, our experiments indicate that when the coupling mode between the jets is switched from out-of-phase to in-phase, the near-field screech peak amplitude increases by about 5 dB for cases where coherence is high. This might suggest a modest degree of screech tone amplification in the in-phase coupling mode. Future single jet experiments will shed light on some of these issues.

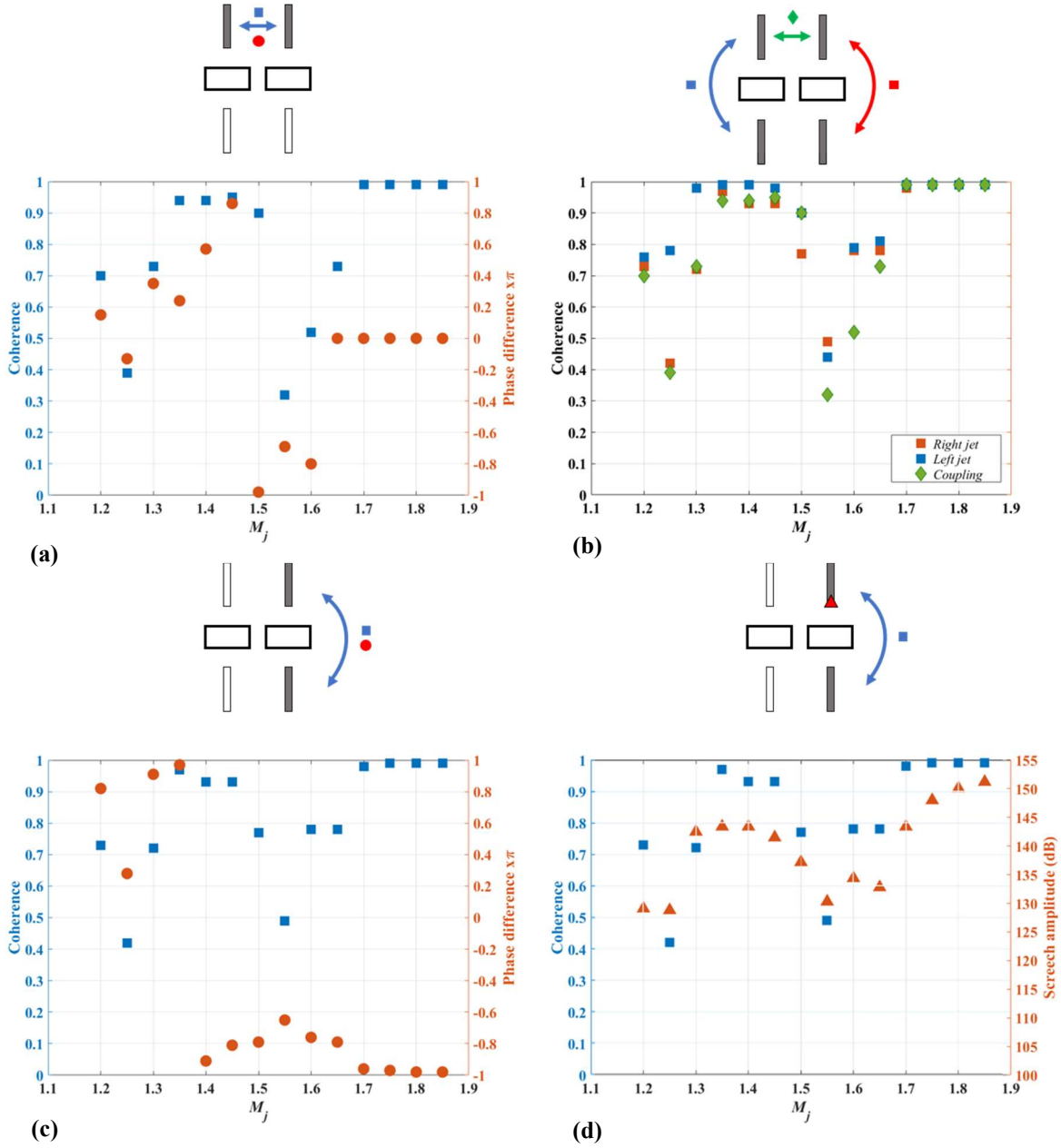

Fig. 7. Twin-jet coupling modes and single jet screech modes observed in the twin rectangular jet setup along the minor axis for a wide range of Mach numbers

To better illustrate the differences between various coupling modes we have observed in the jets, we have selected three cases that are representative of the unique characteristics of each mode for further discussion. M_j = 1.35 represents the coupling characteristics observed in low overexpanded Mach numbers, namely intermittent screech, frequency mismatch and the resultant phase drift. A spectrogram of the signal from microphone 2 is shown in Fig. 8a. The screech peak occurs at St = 0.40 and, as can be seen in the plot, is highly intermittent. This case demonstrates the highest screech peak amplitude in the overexpanded regime (see Fig. 7d). Our results indicate that generally, very high coherence values are accompanied by a steady and consistent phase difference in time. That does not appear to be the case for M_j = 1.35 where, despite high time-averaged coherence values (Fig. 8b), the large error bars on phase values indicate that there are considerable variations in phase in the 0.16s time window of measurements. While the coherence values appear to be consistently high in the measurement window (Fig. 8c), the time-resolved phase plot

(Fig. 8d) indicates that the phase difference between the signals is continuously varying from 0° to -π to +π and back to 0°. The period between instances of time when phase is 0° is approximately 0.030 *s* which corresponds to the frequency difference between the jets: 33 *Hz*. In fact, the frequency mismatch between the jets is the likely reason for the presence of intermittent screech peaks seen in Fig. 8a. This phenomenon is further explained in Fig. 9. Each microphone registers not only the acoustic signature of nearest jet, but that of the other jet as well. Thus, the resultant waveform registered by microphone 2 is the superposition of the jets' acoustic signatures (Fig. 9a). As there is a slight (33 *Hz*) mismatch in screech frequency, the interference between these waveforms generates the beat pattern observed in the spectrogram of microphone 2 signal (see Fig. 9b, same data presented in Fig. 8a). The instances of time where the amplitude of the beat pattern is maximum correspond to a 0° phase difference between the jets and when the difference is ±π, the amplitude of the beat pattern is at its minimum. Raman and Taghavi [11] reported that when two adjacent jets are run simultaneously, they adopt a frequency that is slightly different from the frequency of each jet if it is run individually. They stressed that when jets are coupled, they would always adopt the same frequency. This does not appear to be the case at M_j = 1.35 where despite high coherence (see Fig. 8c), each jet still maintains its own screech frequency. Examining Fig. 7b indicates that each jet has high coherence level which perhaps cannot be overridden by the coupling process.

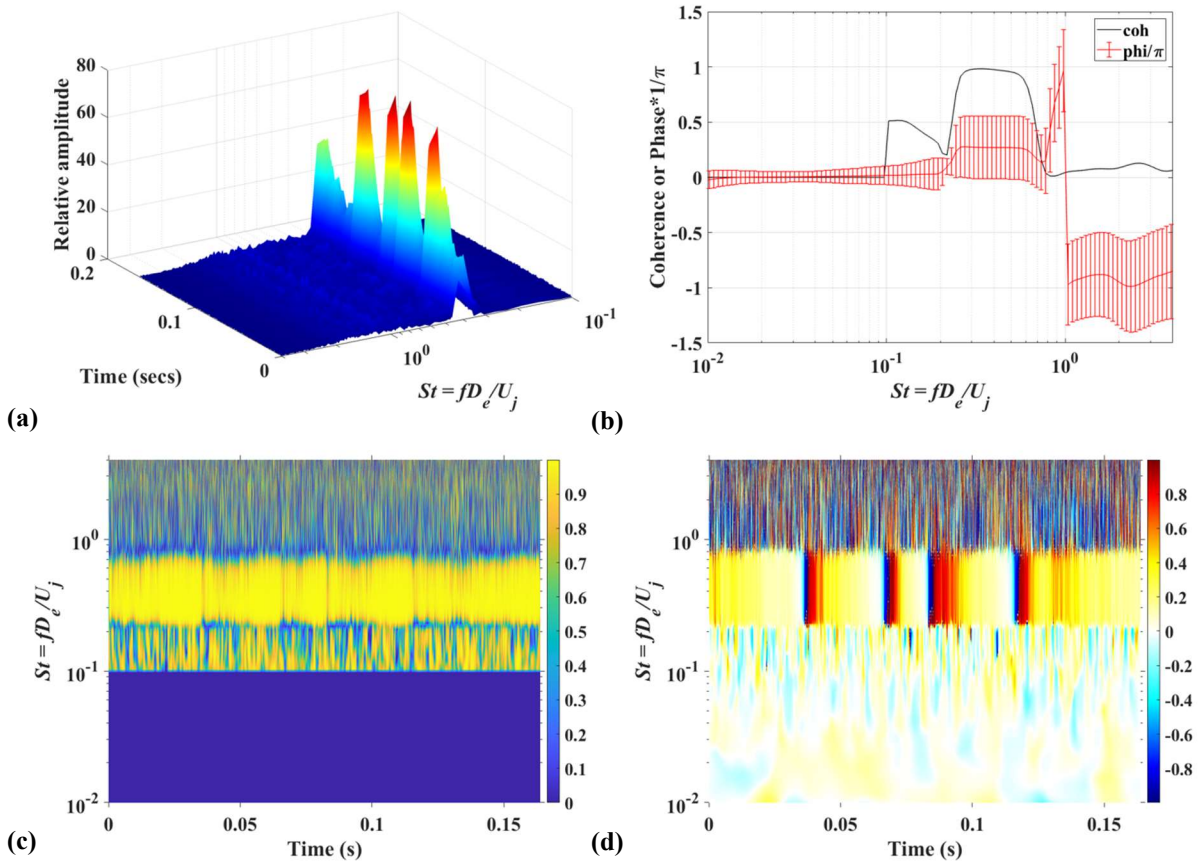

Fig. 8 M_j = 1.35 near-field results from microphones 2 and 3 a) spectrogram of microphone 2 signal, b) time-averaged phase and coherence, c) time-resolved coherence, d) time-resolved phase

The coupling characteristics displayed by M_j = 1.50 are shared by overexpanded Mach numbers that are close to the design Mach number. These characteristics include high coherence values between the jets, low but relatively steady screech peaks and phase difference and the absence of frequency mismatch. As can be seen in Fig. 10a, the relative amplitude of the screech peaks are much lower than those of M_j = 1.35 (see Fig. 8a) as expected in a case where Mach number is the design Mach number, but the intermittency of the peaks is not as pronounced. This is because the previously seen frequency mismatch does not exist at this Mach number.

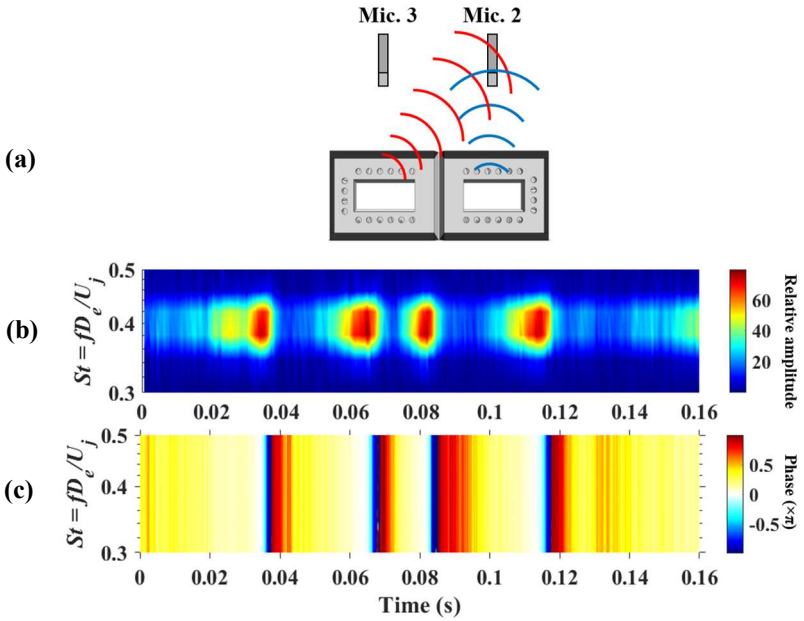

Fig. 9 a) Interference between acoustic waveforms from the jets, b) spectrogram of microphone 2 signal, c) phase difference between microphone 2 and 3

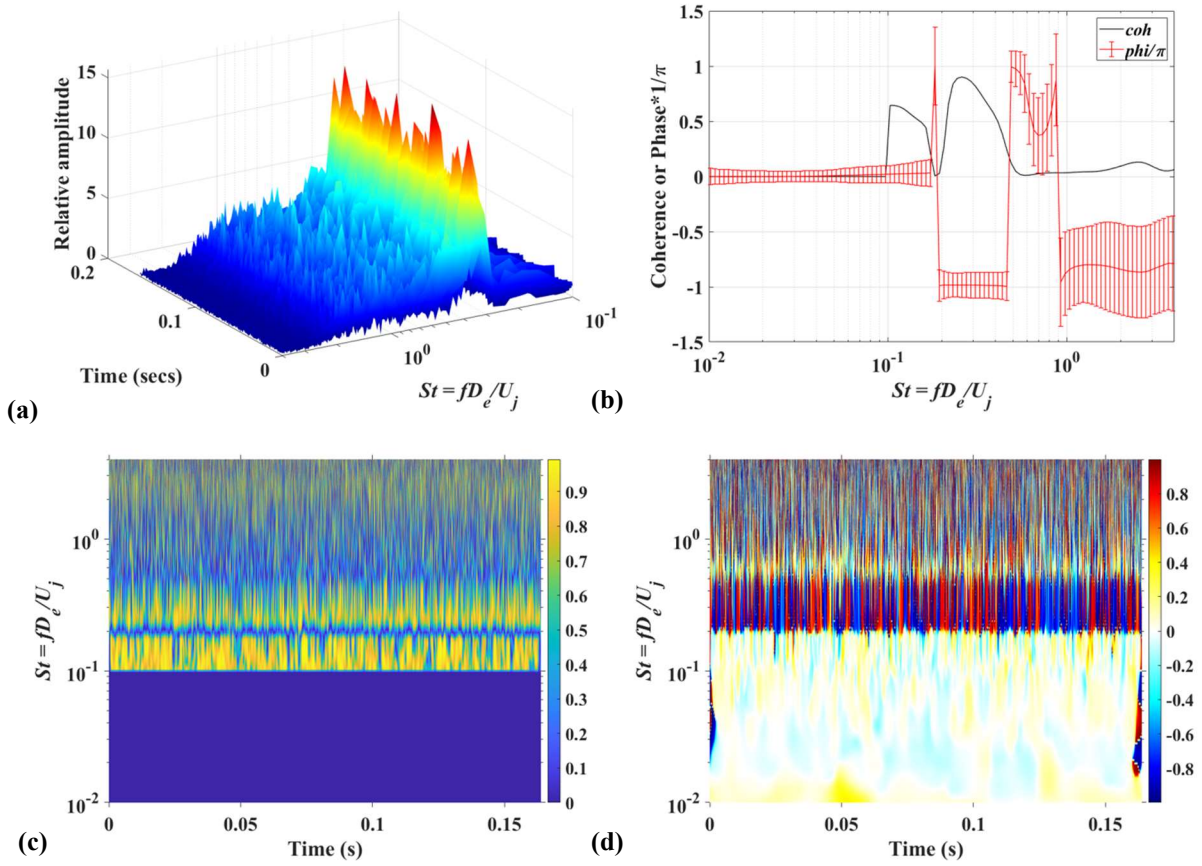

Fig. 10. M_j = 1.50 near-field results from microphones 2 and 3 a) spectrogram of microphone 2 signal, b) time-averaged phase and coherence, c) time-resolved coherence d) time-resolved phase

Fig. 10b shows a strong coherence peak between the signals from microphones 2 and 3 around the screech Strouhal number indicating a consistent and strong coupling between the jets in the minor-axis plane (also see Fig. 10c). The smaller error bars on time-averaged phase at M_j = 1.50 compared to M_j = 1.35 indicate that variations in phase are minimal in time. This is confirmed by the time-resolved phase plot seen in Fig. 10d, which indicates the coupling phase is consistently ±π.This is in part due to the matched frequency of the jets.

Compared to M_j = 1.35 and 1.50, at M_j = 1.70 the screech peaks at St = 0.2 have a higher amplitude and are consistent in time (see Fig. 11a). This Mach number is representative of underexpanded cases with high coherence between the jets (Fig. 11b) indicating a strong, in-phase coupling in the minor-axis plane. As expected, high coherence values are accompanied by a time-consistent phase difference which is evident from the small error bars of time-averaged phase in Fig. 11b and time-resolved phase plot of Fig. 11d. Note that the amplitude of screech peaks at M_j = 1.70 are not significantly higher than that of those at M_j = 1.35 (Fig. 11a vs. Fig. 8a) but the peaks are more consistent. That appears to be the case for all underexpanded Mach numbers between 1.70 and 1.85. Zilz and Wlezien [9], Walker [15] and Raman and Taghavi [11,12] have noted that out-of-phase coupling between the jets results in higher screech peak amplitudes in the near-field compared to in-phase coupling. Our current results indicate that while individual screech peaks at M_j = 1.35 (a case which displays intermittent coupling) are comparable to those observed at M_j = 1.70, the consistency of screech peaks in time is higher in cases where jets are coupled in-phase.

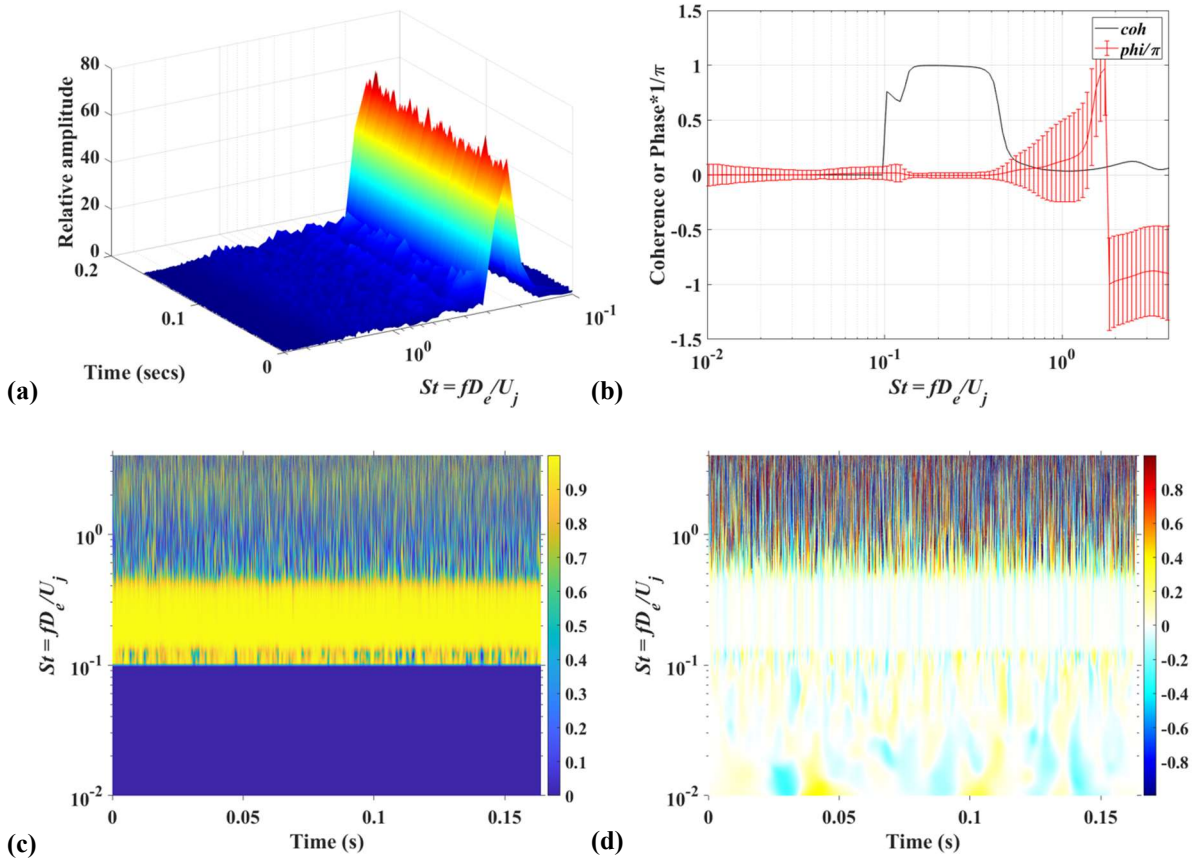

Fig. 11 M_j = 1.70 near-field results from microphones 2 and 3: a) spectrogram of microphone 2 signal, b) time-averaged phase and coherence, c) time-resolved coherence, d) time-resolved phase

2. Far-field Results

Far-field data sets were gathered to characterize the jets' baseline acoustic signature at various nozzle pressure ratios along the major and minor axes (azimuthal angles, φ = 0 and 90°). The three cases representing the various coupling characteristics of the jets, discussed in the previous section, will be examined here so that the effect of near-field coupling dynamics on far-field noise level and directivity can be ascertained. Maps of far-field spectra for a range

of polar angles from θ = 30° – 120°, two different azimuthal angles and three Mach numbers are presented in Fig. 12. Note that θ is measured from the downstream jet axis as shown in Fig. 5.

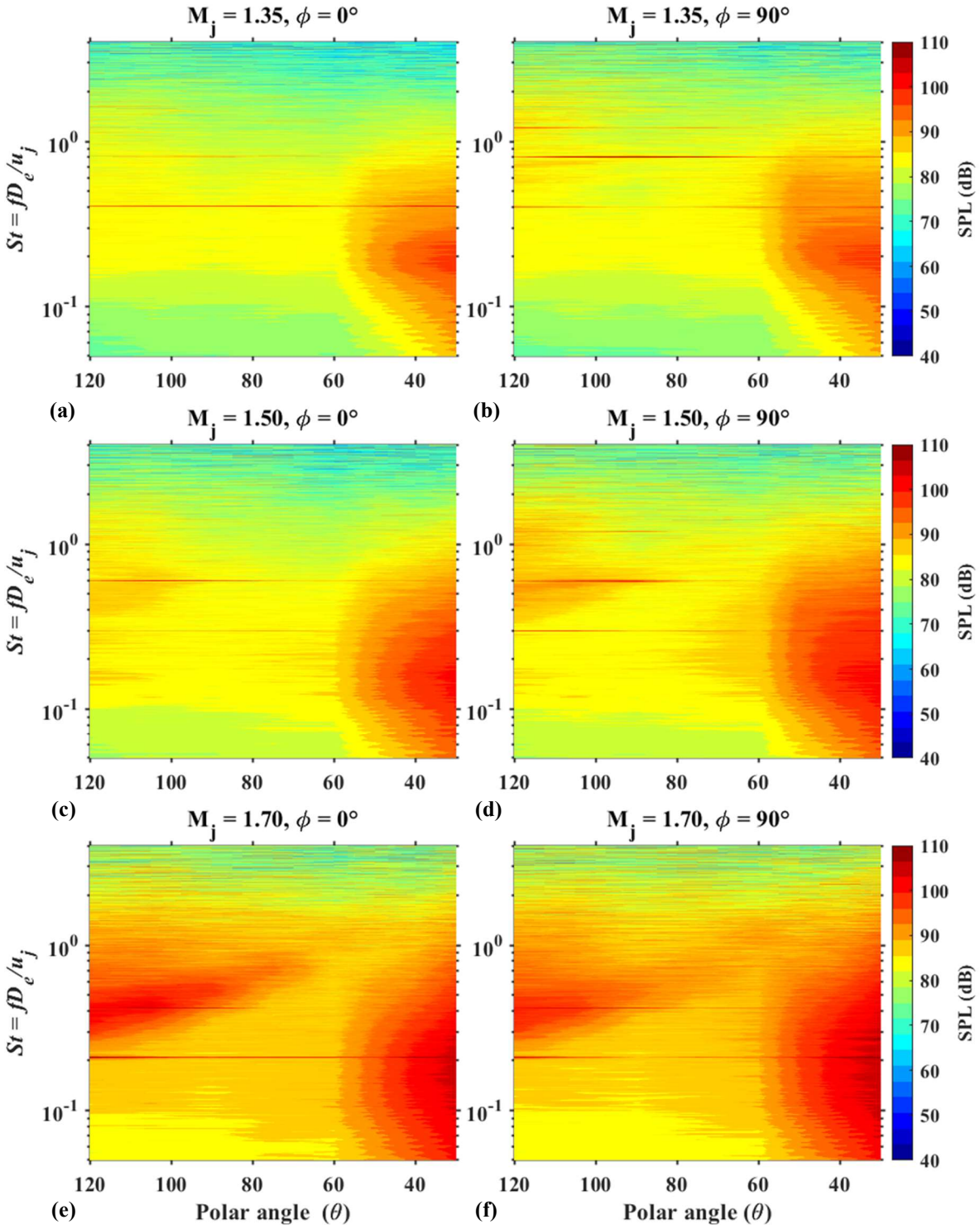

Fig. 12 Maps of far-field SPL for a range of polar angles indicating noise levels and directivity a,b) M_j = 1.35, c,d) M_j = 1.50, e,f) M_j = 1.70

Fig. 12a and b show the far-field spectra for $M_j = 1.35$ along the major and minor axes. Starting with the directivity of the turbulent mixing noise component of the spectra, it appears that the directivity of this component of noise is not strongly dependent on azimuthal angle suggesting that shielding does not play a major role for this component of the noise at this Mach number. This is in line with reports of far-field noise directivity from a geometrically similar setup investigated by Karnam et al. [32]. The mixing noise lobe, however, appears to have a slightly higher peak amplitude along the major axis ($\varphi = 0°$). Although the signature of screech tone (f) is registered strongly at all polar angles along the major axis, it is the first ($2f$) and to some degree second harmonics ($3f$) of the screech that have strong signatures along the minor axis. We can also observe that the 1st harmonic radiates predominantly to the sideline as reported in the literature [37]. At $M_j = 1.35$, which represents an out-of-phase coupling mode, for every complete flapping cycle (observed by far-field microphones between $\theta = 75°$ and 120° for $\varphi = 90°$) the far-field microphones register two flapping events as the jets are not coupled in-phase. Thus, far-field microphones register a strong peak at the first harmonic ($2f$) of the screech fundamental tone along the minor axis (Fig. 12b). This assertion is supported by the fact that the screech mode of the jets at this Mach number is a strong anti-symmetric mode (Fig. 7c). A relatively minor BBSAN peak is only present between $\theta = 100°$ and 120° for $\varphi = 90°$. This feature becomes more dominant as Mach number is increased and is registered along both azimuthal angles at higher Mach numbers. In conclusion, the fact that the amplitudes of screech harmonic tones and peaks of BBSAN are higher along the minor axis compared to those along the major axis at $M_j = 1.35$ reflects the minor axis flapping observed in near-field measurements.

As the Mach number is increased to $M_j = 1.50$, the mixing noise lobe grows in size and amplitude compared to $M_j = 1.35$. While the spreading rate of the jets is higher at lower Mach numbers, as will be discussed in section IV.B, it appears mixing noise levels become higher as Mach number is increased suggesting that the spreading rate of the jets and mixing noise might not be directly related. The high amplitude area of the lobe along the minor axis is larger and more intense (see Fig. 12d) suggesting some effects of acoustic shielding along the major axis. As before, the amplitude of the first and second harmonics of screech are highest along the minor axis between $\theta = 80°$ and 120° reflecting the flapping motion of the jet due to screech. One can also notice a relatively stronger BBSAN lobe at higher frequency than the primary lobe between $\theta = 90°$ and 120° along the minor axis which is absent from the major axis spectra (Fig. 12c and d). This suggests that jet shielding may also hinders the propagation of shock associated noise components. It is also interesting to note the presence of a secondary BBSAN lobe around the second screech harmonic between $\theta = 105°$ and 120° (Fig. 12d).

At $M_j = 1.70$, the screech tone shows a strong downstream directivity and its well-defined peak stands out against the prominent mixing noise lobe for both azimuthal angles (Fig. 12e and f). The mixing noise lobe at $\varphi = 90°$ also shows a wide high-amplitude peak between $St = 0.1$ and 0.3 (Fig. 12f) whereas for $\varphi = 0°$, the high-amplitude lobe is somewhat smaller suggesting a possible shielding effect in propagation of mixing noise component at this Mach number. It is interesting to note that at $M_j = 1.70$, in contrast to the previous cases, the signature of the screech primary tone and its harmonic are stronger along the major axis. This is rather unexpected as the jets are strongly coupled in-phase at this Mach number and based on the existing reports in the literature [9,11,15] one might expect to observe higher noise levels along the minor axis normal to the twin-jet plane. Another observation from the results acquired along the major axis is that the high-amplitude broadband peaks between $St = 0.3$ and 0.5 stretch from $\theta = 90°$ to $\theta = 120°$ whereas along the minor axis, the broadband lobe is only dominant between $\theta = 105°$ and 120°. In short, the trends in far-field noise directivity indicate that at $M_j = 1.35$ and 1.50, mixing noise appears to be the dominant noise component and the amplitude of the screech tones is highest along the minor axis. At $M_j = 1.70$, however, in an unexpected turn, the amplitude of the screech tone and its first harmonic become higher along the major axis and BBSAN becomes a significant source of noise on par with turbulent mixing noise.

As active flow control strategies for addressing different components of far-field noise are dissimilar, the insights gained from examining the maps of far-field noise are invaluable and would assist us in the process of choosing the excitation parameters for implementing active control.

B. Optical Diagnostics

1. Time-averaged Schlieren

In order to further complement the insights gained from near- and far-field acoustic measurements, an extensive schlieren imaging campaign was conducted. High-resolution images of the jets along the minor and major axes were acquired for Mach numbers between 1.20 and 1.90 in increments of 0.05. In this section, a limited set of results for the Mach numbers that have been selected for discussion are presented. In the course of our investigation of twin-jet flow-field, we noticed the presence of standing waves at some specific Mach numbers. In order to further discuss

standing waves, a brief background is presented here. Panda [38] reported the presence of standing waves (SWs) in an underexpanded axisymmetric jet for the first time and attributed their presence to an interference between downstream propagating hydrodynamic waves just outside of the jet (signature of large-scale structures convecting downstream in the shear layer of the jet) and upstream propagating acoustic waves. He argued that the correct length scale in Powell's screech formula [39] is SW wavelength. This postulate would give the formation of standing waves a key role in the generation of screech, and potentially the resultant coupling phenomenon. Accordingly, an understanding of the presence and role of standing waves in the rectangular twin-jet flow field is an important part of the overall understanding of the dynamics necessary to effectively implement flow control.

Panda managed to identify standing waves by obtaining maps of root mean square of pressure fluctuations. An alternative approach to identifying standing waves was proposed by Edgington-Mitchell et al. [40], which involved calculating the standard deviation of intensity values from sets of schlieren images. Bell et al. [41] later on visualized standing waves in their particle image velocimetry (PIV) data by calculating Log_{10} of standard deviation from maps of axial velocity. Aside from providing a length scale that can be used to predict screech frequency, the importance of the SWs lies in the fact that their presence might be tied to the dynamics of coupling between the jets. By comparing the Mach numbers at which standing waves were present against a plot of coherence level of screech for a single jet (Fig. 7d), we noticed that standing waves appear whenever the coherence level of screech is rising, i.e. M_j = 1.20 – 1.35 and 1.65 – 1.80. Whenever coherence and amplitude attain their maximum values for each flow regime, i.e. overexpanded and underexpanded, standing waves tend to disappear. We have not been able to find any reports in the literature that tie the existence of standing waves to the coherence level of screech and believe this might be the first account of such a relationship. Furthermore, none of the investigations in which standing waves have been addressed [38,40–42] have been conducted using a rectangular nozzle. Therefore, more research is warranted to provide a better understanding of these issues.

Maps of streamwise intensity gradients and Log_{10} of standard deviation of intensity gradients acquired along the major axis of the twin-jet assembly are presented in Fig. 14 while Fig. 15 shows maps of Log_{10} of standard deviation of intensity gradients along the minor axis. Fig. 14a shows a M_j = 1.35 jet which is representative of the coupling characteristics observed in low overexpanded Mach numbers. As was shown in Fig. 7a, b and d, the coherence level of screech is quite high at this Mach number and the screech amplitude is highest among the overexpanded Mach numbers. Furthermore, the coherence of signals from microphones located above the jets is high indicating strong coupling between the jets (see Fig. 8b and c). Several observations can be made from examining Fig. 14a. First, the centerline fluctuations begin to decrease monotonically at approximately $6D_e$. This location is likely to be the end of the potential core where coherent structures break down and dissipate. Next, as Panda reported, there is a mismatch between the location of the shock cell tips and the crests of the standing wave lobes [38]. While the crests sometimes are nearly aligned with the shock cell tips (Fig. 14a, x/D_e = 1.8), in general they fall somewhere between the cell tips. According to Panda, significant pressure differences between the crest and the trough of the SWs exist along the jet boundary [38]. At M_j = 1.35, there is a ∼20% difference in intensity fluctuation levels between the crest of the lobe and its trough (see Fig. 14a).

Panda indicated that the SW pattern is three dimensional and usually would be wrapped around an axisymmetric jet [38]. Knast et al. [42] observed the presence of SWs in a twin circular jet setup when the jets were viewed along the twin-jet plane and normal to it. Examining Figs. 15a, b and c indicates that SWs are never present when the jets are viewed along their minor axis. As mentioned previously, we did not detect evidence of presence of a screech loop in the horizontal plan and high-speed schlieren imaging experiments did not show any lateral motion of the jets due to shedding of vortical structures along the minor axis of the jet, as a result, the ingredients needed for the presence of standing waves in the horizontal plan are non-existent.

We noticed that as the Mach number is increased from M_j = 1.35, the standing waves disappear and do not emerge again until M_j = 1.65 (not shown here). Fig. 14b confirms the absence of standing waves at M_j = 1.50. The furthest axial location displaying the maximum value of intensity fluctuation is now x/D_e = 7 indicating that the potential core length has increased compared to M_j = 1.35. The spreading angle of the jet in the minor axis plane has also been reduced. For M_j = 1.35, the edge of the jet at x/D_e = 9 is approximately at z/D_e = 2.9. For M_j = 1.50, however, at the same axial location, the edge of the jet lines up with z/D_e = 2.3. That corresponds to a 20.7% lower spreading rate for M_j = 1.50 (Fig. 14b).

Following the reemergence of standing waves at M_j = 1.65, the lobes become well-defined and dominate the near-field at M_j = 1.70. For this case, the furthest axial location of maximum intensity fluctuation is at x/D_e = 8.2. There is a 9.7% difference between the value of intensity fluctuations between the crest located at x/D_e = 3.4 and the adjacent trough at x/D_e = 4.7. Due to the presence of standing waves, it is not possible to exactly measure the jet's spreading angle in the minor axis plane at M_j = 1.70, however, it appears that the jets spreading angle has not significantly changed compared to M_j = 1.70. As reported by Shih et al. [34] and Alkislar et al. [3], the maximum spreading rate of

the jet occurs when the jets are flapping out-of-phase. The wavelength of the standing waves, on other hand, has been increased compared to M_j = 1.35. For M_j = 1.35, the spacing between the crests is approximately $1D_e$ whereas for M_j = 1.70, it is close to $2D_e$. These increases appear to be comparable to growths in shock cell length going from M_j = 1.35 to 1.70. This is in line with observations of Knast et al. [42] in a twin circular jet setup where they reported that changes in wavelength of standing waves closely follows those of shock cell spacing. Panda's observations from a converging single circular nozzle[38], however, were not similar.

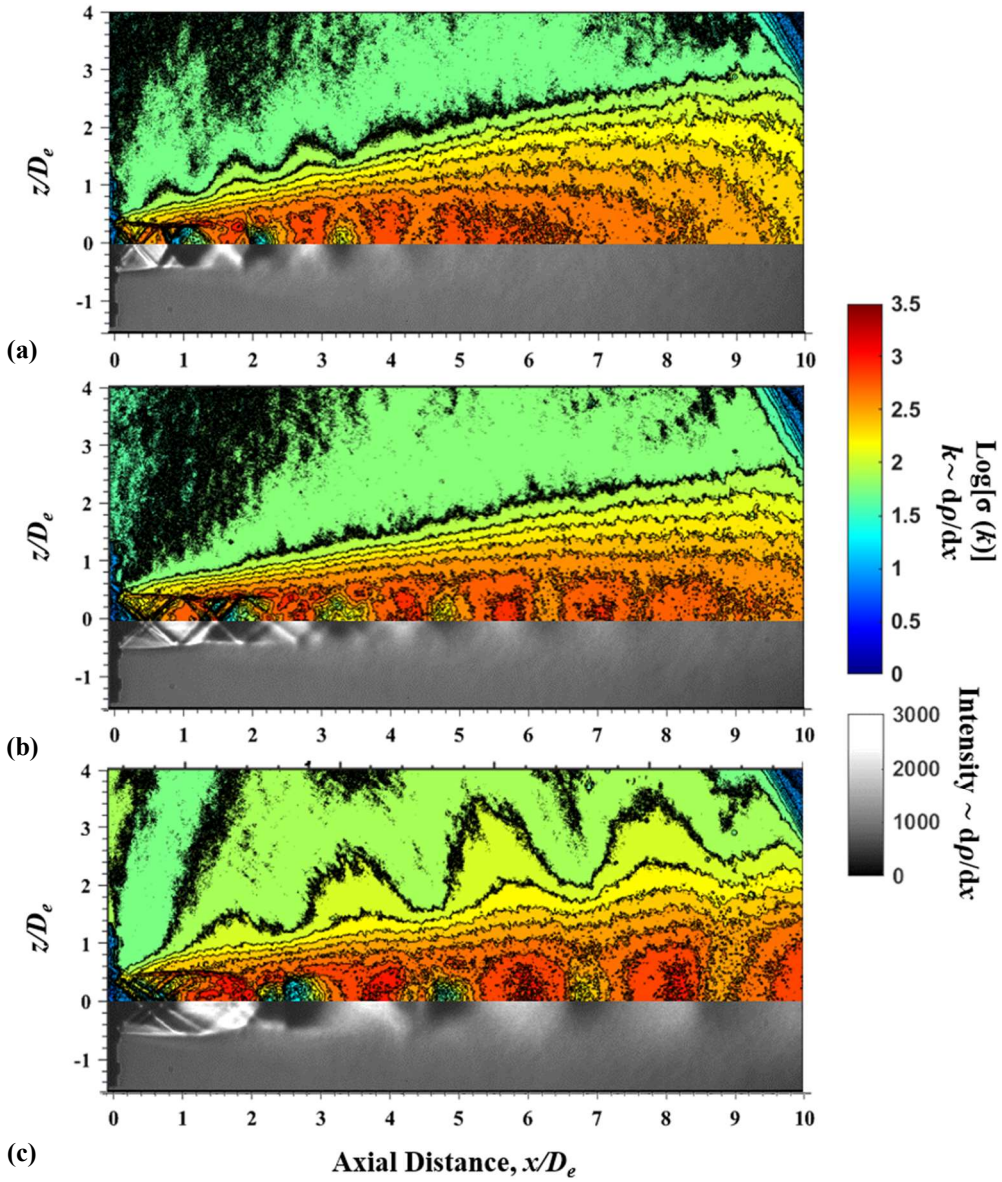

Fig. 14 Maps of Log[σ(*k*)] where *k* ~ d*ρ*/d*x* (top) and schlieren images (sensitive to axial density gradients d*ρ*/d*x*) (bottom) for a) M_j = 1.35, b) M_j = 1.50, c) M_j = 1.70

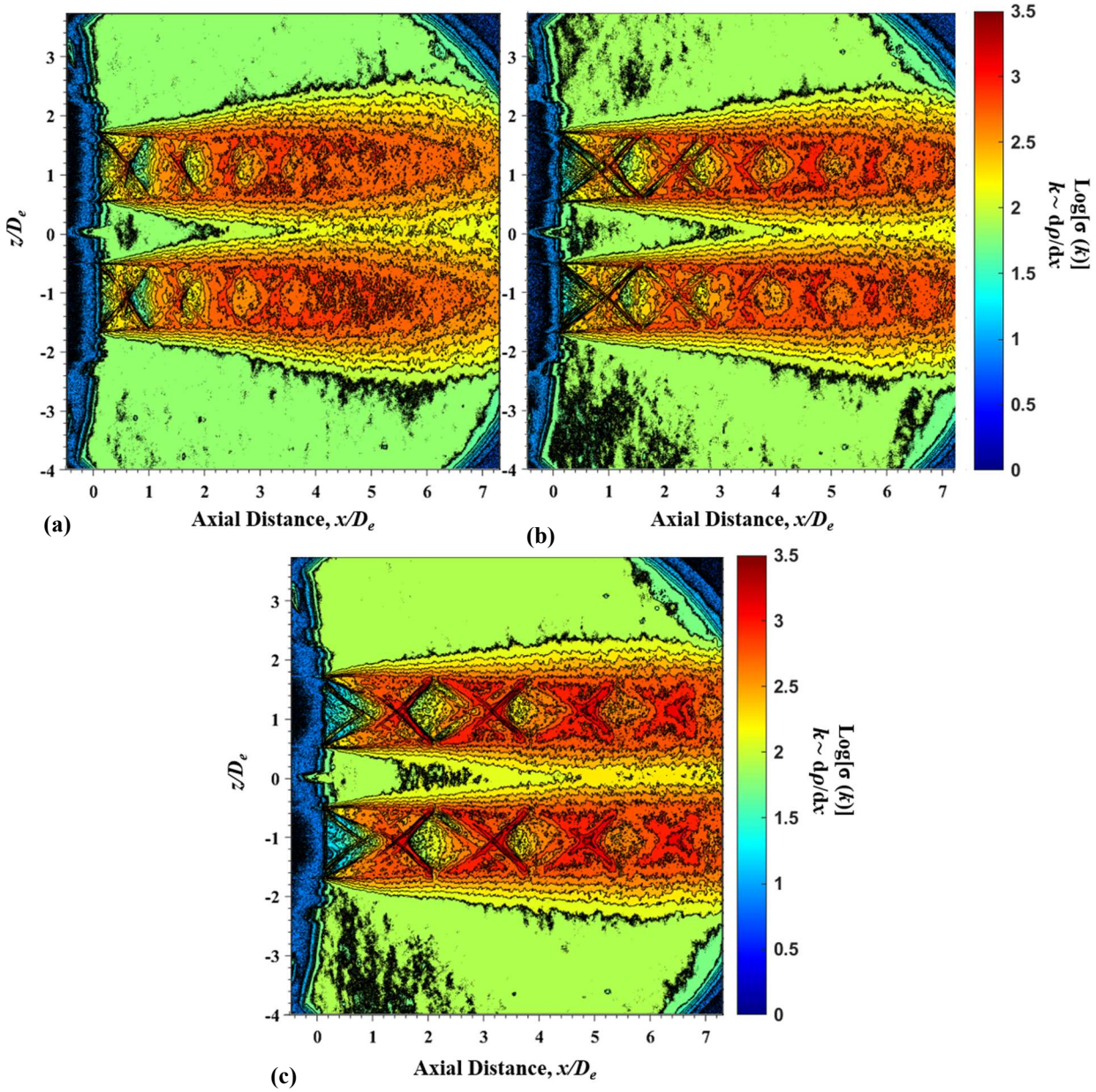

Fig. 15 Maps of Log[σ(*k*)] where $k \sim d\rho/dx$ for a) $M_j = 1.35$, b) $M_j = 1.50$, c) $M_j = 1.70$

V. Conclusions

A new, low aspect ratio, twin rectangular jet assembly has been designed, constructed and tested across a wide range of fully expanded jet Mach numbers to gain a thorough understanding of the coupling modes of the jets and the effects of those modes on near-field sound pressure levels and far-field noise directivity. The insights gained will aid in implementing active flow control for noise reduction and decoupling the jets in the upcoming experiments at the Gas Dynamics and Turbulence Laboratory. When comparing the normalized screech frequencies from our facility with the results of other researchers using rectangular nozzles with low to moderate aspect ratios ($AR = 2$ to 5) reported in the literature, we noticed that area-based equivalent diameter (D_e), not nozzle height h, collapsed the screech data.

Wavelet coherence and phase between near-field acoustic measurements were used to investigate the screech and coupling modes of the twin-jets at various Mach numbers. The results indicate that each individual jet always adopts

an anti-symmetric (flapping) screech mode regardless of the Mach number. The screech amplitude and coherence are reduced at Mach numbers close to the design Mach number. A frequency mismatch was observed at low overexpanded Mach numbers, which led to intermittent screech peaks and a phase drift between the jets. As the Mach number increases, the frequency mismatch disappears and the strength of the screech amplitude increases. Coupling in overexpanded Mach numbers in the vicinity of the design Mach number is out-of-phase while in the majority of underexpanded cases, the jets are strongly coupled in-phase. Better understanding these dynamics will be crucial to effectively implementing instability-leveraging flow control to control the jet coupling.

Dynamics of coupling in the near-field affect noise directivity patterns in the far-field. Far-field acoustic measurements were conducted for azimuthal angles of $\varphi = 0°$ and 90° and polar angles ranging from $\theta = 30°$ to 120°. The amplitude of the BBSAN components in the far-field were found to be higher along the minor axis for $M_j = 1.35$ and 1.50 whereas for $M_j = 1.70$, this trend is reversed. Turbulent mixing noise is the dominant noise component at $M_j = 1.35$ and 1.50. At $M_j = 1.70$, however, BBSAN amplitude approaches that of mixing noise. Flow-field visualizations with a standard Z-type schlieren system revealed that standing waves are present at Mach numbers where strength of the screech loop and screech amplitude was increasing. More work is needed to investigate and understand the underlying reasons for the presence of standing waves.

Acknowledgements

The support of this research by the Office of Naval Research under contract No. N00014-19-1-2207 through Dr. Steve Martens is gratefully acknowledged. Fruitful discussions with Dr. John Spyropoulos of NAVAIR are very much appreciated. We would also like to thank Andrew Sais and Jack Tyszkiewicz for their assistance in setting up the schlieren system and post-processing the near-field acoustic data.

References

[1] Dusa, D., Speir, D., Rowe, R., and Leavitt, L. Advanced Technology Exhaust Nozzle Development. In *19th Joint Propulsion Conference*, AIAA paper 1983-1286, June 1983.

[2] Wiegand, C. F-35 Air Vehicle Technology Overview. In *2018 Aviation Technology, Integration, and Operations Conference*, AIAA paper 2018-3368, June 2018

[3] Alkislar, M. B., Krothapalli, A., and Lourenco, L. M. "Structure of a Screeching Rectangular Jet: A Stereoscopic Particle Image Velocimetry Study." *Journal of Fluid Mechanics*, Vol. 489, 2003, pp. 121–154. https://doi.org/10.1017/S0022112003005032.

[4] Krothapalli, A., Baganoff, D., and Karamcheti, K. "On the Mixing of a Rectangular Jet." *Journal of Fluid Mechanics*, Vol. 107, 1981, pp. 201–220. https://doi.org/10.1017/S0022112081001730.

[5] Mixson, J. S., and Roussos, L. A. Acoustic Fatigue: Overview of Activities at NASA Langley. *NASA Technical Memorandum* NTM-89143, April 1987.

[6] Berndt, D. E. Dynamic pressure fluctuations in the internozzle region of a twin-jet nacelle. No. 841540. SAE Technical Paper, 1984.

[7] Shaw, L. "Twin-Jet Screech Suppression." *Journal of Aircraft*, Vol. 27, No. 8, 1990, pp. 708–715. https://doi.org/10.2514/3.25344.

[8] Harper-Bourne, M. Twin-Jet near-Field Noise Prediction. In *6th Aeroacoustics Conference and Exhibit*, AIAA paper 2000-2084, June 2000.

[9] Zilz, D., and Wlezien, R. The Sensitivity of Near-Field Acoustics to the Orientation of Twin Two-Dimensional Supersonic Nozzles. In *26th Joint Propulsion Conference*, AIAA paper 1990-2149, July 1990.

[10] Zeierman, S., Gutmark, E., and Nosseir, N. Characteristics of Two Adjacent Rectangular Jets. In *30th Aerospace Sciences Meeting and Exhibit*, AIAA paper 1992-237, January 1992.

[11] Raman, G., and Taghavi, R. "Coupling of Twin Rectangular Supersonic Jets." *Journal of Fluid Mechanics*, Vol. 354, 1998, pp. 123–146. https://doi.org/10.1017/S0022112097007441.

[12] Raman, G., and Taghavi, R. "Resonant Interaction of a Linear Array of Supersonic Rectangular Jets: An Experimental Study." *Journal of Fluid Mechanics*, Vol. 309, 1996, pp. 93–111. https://doi.org/10.1017/S0022112096001577.

[13] Bozak, R. Twin Jet Effects on Noise of Round and Rectangular Jets: Experiment and Model. In *20th AIAA/CEAS Aeroacoustics Conference*, AIAA paper 2014-2890, June 2014.

[14] Bozak, R., and Wernet, M. P. Subsonic Round and Rectangular Twin Jet Flow Effects. In *50th AIAA/ASME/SAE/ASEE Joint Propulsion Conference*, AIAA paper 2014-3736, July 2014.
[15] Walker, S. Twin Jet Screech Suppression Concepts Tested for 4.7 Percent Axisymmetric and Two-Dimensional Nozzle Configurations. In *26th Joint Propulsion Conference*, AIAA paper 90-2150, July 1990.
[16] Kuo, C.-W., Cluts, J., and Samimy, M. "Exploring Physics and Control of Twin Supersonic Circular Jets." *AIAA Journal*, Vol. 55, No. 1, 2017, pp. 68–85. https://doi.org/10.2514/1.J054977.
[17] Karnam, A., Baier, F., and Gutmark, E. J. Nature of Flow Field & Acoustics of Twin Supersonic Rectangular Jets. In *AIAA Scitech 2020 Forum*, AIAA paper 2020-0500, January 2020.
[18] Kalagotla, D., Karnam, A., and Gutmark, E. J. Comparison of Flow Characteristics of Single and Twin Rectangular Jets Using OVERFLOW Code. In *AIAA Scitech 2020 Forum*, AIAA paper 2020-1334, January 2020.
[19] Viswanath, K., Liu, J., Ramamurti, R., Karnam, A., Baier, F., and Gutmark, E. J. Noise Characteristics of Low Aspect Ratio Supersonic Twin Jet Configuration. In *AIAA Scitech 2020 Forum*, AIAA paper 2020-0496, January 2020.
[20] Utkin, Y. G., Keshav, S., Kim, J.-H., Kastner, J., Adamovich, I. V., and Samimy, M. "Development and Use of Localized Arc Filament Plasma Actuators for High-Speed Flow Control." *Journal of Physics D: Applied Physics*, Vol. 40, No. 3, 2007, pp. 685–694. https://doi.org/10.1088/0022-3727/40/3/S06.
[21] Samimy, M., Adamovich, I., Webb, B., Kastner, J., Hileman, J., Keshav, S., and Palm, P. "Development and Characterization of Plasma Actuators for High-Speed Jet Control." *Experiments in Fluids*, Vol. 37, No. 4, 2004, pp. 577–588. https://doi.org/10.1007/s00348-004-0854-7.
[22] Samimy, M., Webb, N., and Crawley, M. "Excitation of Free Shear-Layer Instabilities for High-Speed Flow Control." *AIAA Journal*, Vol. 56, No. 5, 2018, pp. 1770–1791. https://doi.org/10.2514/1.J056610.
[23] Samimy, M., Kim, J.-H., Kastner, J., Adamovich, I., and Utkin, Y. "Active Control of High-Speed and High-Reynolds-Number Jets Using Plasma Actuators." *Journal of Fluid Mechanics*, Vol. 578, 2007, pp. 305–330. https://doi.org/10.1017/S0022112007004867.
[24] Samimy, M., Kearney-Fischer, M., and Kim, J.-H. "High-Speed and High-Reynolds-Number Jet Control Using Localized Arc Filament Plasma Actuators." *Journal of Propulsion and Power*, Vol. 28, No. 2, 2012, pp. 269–280. https://doi.org/10.2514/1.B34272.
[25] Esfahani, A., Webb, N., and Samimy, M. "Flow Separation Control over a Thin Post-Stall Airfoil: Effects of Excitation Frequency." *AIAA Journal*, Vol. 57, No. 5, 2019, pp. 1826–1838. https://doi.org/10.2514/1.J057796.
[26] Yugulis, K., Hansford, S., Gregory, J. W., and Samimy, M. "Control of High Subsonic Cavity Flow Using Plasma Actuators." *AIAA Journal*, Vol. 52, No. 7, 2014, pp. 1542–1554. https://doi.org/10.2514/1.J052668.
[27] Webb, N., and Samimy, M. "Control of Supersonic Cavity Flow Using Plasma Actuators." *AIAA Journal*, Vol. 55, No. 10, 2017, pp. 3346–3355. https://doi.org/10.2514/1.J055720.
[28] Samimy, M., Webb, N., and Esfahani, A. "Reinventing the Wheel: Excitation of Flow Instabilities for Active Flow Control Using Plasma Actuators." *Journal of Physics D: Applied Physics*, Vol. 52, No. 35, 2019, p. 354002. https://doi.org/10.1088/1361-6463/ab272d.
[29] Hahn, C., Kearney-Fischer, M., and Samimy, M. "On Factors Influencing Arc Filament Plasma Actuator Performance in Control of High Speed Jets." *Experiments in Fluids*, Vol. 51, 2011, pp. 1591–1603. https://doi.org/10.1007/s00348-011-1172-5.
[30] Gutmark, E., Schadow, K. C., and Bicker, C. J. "Near Acoustic Field and Shock Structure of Rectangular Supersonic Jets." *AIAA Journal*, Vol. 28, No. 7, 1990, pp. 1163–1170. https://doi.org/10.2514/3.25187.
[31] Raman, G., and Rice, E. J. "Instability Modes Excited by Natural Screech Tones in a Supersonic Rectangular Jet." *Physics of Fluids*, Vol. 6, No. 12, 1994, pp. 3999–4008. https://doi.org/10.1063/1.868389.
[32] Karnam, A., Baier, F., and Gutmark, E. J. Near Field Acoustic Analysis of Cold Supersonic Rectangular Jets. In *AIAA Scitech 2019 Forum*, AIAA paper 2019-0809, January 2019.
[33] Jeun, J., Wu, G. J., and Lele, S. K. Towards Large-Eddy Simulations of Twin Rectangular Jets Including Screech. In *AIAA Scitech 2020 Forum*, AIAA paper 2020-0998, January 2020.
[34] Shih, C., Krothapalli, A., and Gogineni, S. "Experimental Observations of Instability Modes in a Rectangular Jet." *AIAA Journal*, Vol. 30, No. 10, 1992, pp. 2388–2394. https://doi.org/10.2514/3.11238.
[35] Panda, J., Raman, G., Zaman, K., Panda, J., Raman, G., and Zaman, K. Underexpanded Screeching Jets from Circular, Rectangular and Elliptic Nozzles. In *3rd AIAA/CEAS Aeroacoustics Conference*, American Institute of Aeronautics and Astronautics.
[36] Raman, G. "Cessation of Screech in Underexpanded Jets." *Journal of Fluid Mechanics*, Vol. 336, 1997, pp. 69–90. https://doi.org/10.1017/S002211209600451X.

[37] Tam, C. K. W. “Supersonic Jet Noise.” *Annual Review of Fluid Mechanics*, Vol. 27, No. 1, 1995, pp. 17–43. https://doi.org/10.1146/annurev.fl.27.010195.000313.
[38] Panda, J. “An Experimental Investigation of Screech Noise Generation.” *Journal of Fluid Mechanics*, Vol. 378, 1999, pp. 71–96. https://doi.org/10.1017/S0022112098003383.
[39] Powell, A. “On the Noise Emanating from a Two-Dimensional Jet Above the Critical Pressure.” *The Aeronautical Quarterly*, Vol. 4, No. 2, 1953, pp. 103–122. https://doi.org/10.1017/S0001925900000822.
[40] Edgington-Mitchell, D., Honnery, D. R., and Soria, J. “Staging Behaviour in Screeching Elliptical Jets:” *International Journal of Aeroacoustics*, 14(7), 2015, pp.1005-1024. https://doi.org/10.1260/1475-472X.14.7.1005.
[41] Bell, G., Soria, J., Honnery, D., and Edgington-Mitchell, D. “An Experimental Investigation of Coupled Underexpanded Supersonic Twin-Jets.” *Experiments in Fluids*, Vol. 59, No. 9, 2018, p. 139. https://doi.org/10.1007/s00348-018-2593-1.
[42] Knast, T., Bell, G., Wong, M., Leb, C. M., Soria, J., Honnery, D. R., and Edgington-Mitchell, D. “Coupling Modes of an Underexpanded Twin Axisymmetric Jet.” *AIAA Journal*, Vol. 56, No. 9, 2018, pp. 3524–3535. https://doi.org/10.2514/1.J056434.